Formation and Maturation of Parallel Fiber-Purkinje Cell Synapses in the Staggerer Cerebellum Ex Vivo

Janmaat, Sonja; Frederic, Florence; Sjollema, Klaas; Luiten, Paul; Mariani, Jean; van der Want, Johannes

Published in:
Journal of comparative neurology

DOI:
10.1002/cne.21910

The Journal of Comparative Neurology 512:467–477 (2009)

Formation and Maturation of Parallel Fiber-Purkinje Cell Synapses in the *Staggerer* Cerebellum Ex Vivo

SONJA JANMAAT,[1–3] FLORENCE FRÉDÉRIC,[3] KLAAS SJOLLEMA,[1] PAUL LUITEN,[2] JEAN MARIANI,[3,4] AND JOHANNES VAN DER WANT[1]*

[1]Department of Cell Biology; Molecular Imaging and Electron Microscopy, University Medical Center Groningen, University of Groningen, The Netherlands

[2]Department of Molecular Neurobiology, University of Groningen, The Netherlands

[3]Neurobiologie des Processus Adaptatifs, Equipe Développement et Vieillissement du Système Nerveux, CNRS-UMR 7102, Paris, France

[4]APHP, Hôpital Charles Foix, UEF, Ivry sur Seine, France

ABSTRACT

In vivo, homozygous *staggerer* (*Rora*$^{sg/sg}$) Purkinje cells (PCs) remain in an early stage of development with rudimentary spineless dendrites, associated with a lack of parallel fiber (PF) input and the persistence of multiple climbing fibers (CFs). In this immunocytochemical study we used cerebellar organotypic cultures to monitor the development of *Rora*$^{sg/sg}$ PF-PC synapses in the absence of CF innervation. Ex vivo the vesicular glutamate transporters VGluT1 and VGluT2 reactivity was preferentially localized around the *Rora*$^{sg/sg}$ PC soma and proximal dendrites, which are typically CF domains. The shift from VGluT2 to VGluT1 in PF terminals during development was delayed in *Rora*$^{sg/sg}$ slices. The postsynaptic receptors mGluR1 and GluRδ2 were differently distributed on *Rora*$^{sg/sg}$ PCs. mGluR1 reactivity was evenly distributed in PC soma and dendrites, whereas GluRδ2 reactivity, normally restricted at PF synapses, was dense in *Rora*$^{sg/sg}$ PC somata. The presynaptic distribution of VGluT1 and VGluT2 on *Rora*$^{sg/sg}$ PCs matched the postsynaptic distribution of the glutamate receptor GluRδ2, but not mGluR1. J. Comp. Neurol. 512: 467–477, 2009. © 2008 Wiley-Liss, Inc.

Indexing terms: Purkinje cells; parallel fiber; *Rora*$^{sg/sg}$; *VGluT1 and VGluT2*

The formation of neuronal networks in the cerebellum, in particular the wiring of the Purkinje cell (PCs), has been widely studied. Activities of two excitatory afferents, climbing fibers (CFs) and parallel fibers (PFs), underlie the plasticity of PC synapses, inducing cerebellar long-term depression (LTD) and permitting cerebellar motor learning (Crepel, 1982; Ito, 1989; Linden and Connor, 1995). After the formation of first CF-PC, and then PF-PC synapses, connections are dynamically modified, resulting in the elimination of supernumerary CFs and the establishment of the one-to-one CF-PC relationship, in parallel with ongoing synaptogenesis onto PCs from PFs (Eccles et al., 1966; Crepel et al., 1976; Mariani and Changeux, 1981; Chedotal and Sotelo, 1992; Sotelo, 2004). These two processes are profoundly disturbed in the *staggerer* mutant mouse (Sotelo and Privat, 1978; Bradley and Berry, 1978; Crepel et al., 1980; Mariani and Changeux, 1980; Sotelo, 1990).

The *staggerer* mutation, a deletion in the ligand binding domain of the *Rora* gene (Retinoic acid receptor-related Orphan Receptor) (Sidman et al., 1962; Hamilton et al., 1996), leads to massive degeneration of cerebellar neurons from early postnatal age (Sidman et al., 1962; Sotelo and Changeux, 1974; Herrup, 1983; Vogel et al., 2000; Doulazmi et al., 2001). In adult *Rora*$^{sg/sg}$ mice, the surviving PCs (about 15%) remain in an early stage of development, with rudimentary spineless dendrites, associated with almost complete absence of PF synapses and the persistence of multiple CF innervations (Crepel et al., 1980; Mariani, 1982; Boukhtouche et al., 2006a; Gold et al., 2007). We have previously shown that, in organotypic cerebellar cultures, *Rora*$^{sg/sg}$ PCs also remain in an immature developmental stage and that induction of hRORα1 protein within them is sufficient to restore a cell-autonomous process of spinogenesis (Boukhtouche et al., 2006b).

Little is known, however, about the organization of pre- and postsynaptic elements during the formation of PF synapses on *Rora*$^{sg/sg}$ PC somata and dendrites. Here we studied the establishment of PF-PC connectivity by examining ex vivo the localization of presynaptic vesicular glutamate transporters 1

*Correspondence to: J.J.L. van der Want, Department of Cell Biology; Molecular Imaging and Electron Microscopy, University Medical Center Groningen, University Groningen, Antonius Deusinglaan 1, 9713 AV Groningen, The Netherlands. E-mail: j.j.l.van.der.want@med.umcg.nl

Received 18 March 2008; Revised 7 August 2008; Accepted 15 October 2008

DOI 10.1002/cne.21910

Published online in Wiley InterScience (www.interscience.wiley.com).

and 2 (VGluT1 and VGluT2) and of postsynaptic glutamate receptors mGluR1 and GluRδ2. In vivo, PF terminals express predominantly VGluT2 during the first 10 postnatal days and then switch to VGluT1 with further maturation (Miyazaki et al., 2003). GluRδ2 is required for consolidating PF synapses, whereas both GluRδ2 and the mGluR1-signaling pathway are involved in eliminating redundant CF synapses at the proximal dendrites (for recent reviews, see Hirano, 2006; Gounko et al., 2007). We used organotypic cerebellar cultures from postnatal day (P)0 pups, an age when most CF-PC connections have not yet been established, and kept them for 7, 14, and 21 days in vitro (DIV). Organotypic slice cultures are an established method to study many aspects of neural development and function of the cerebellum in the absence of mossy and climbing fiber afferents (Tanaka et al., 1994; Dusart et al., 1997). The preservation of the intracerebellar neuronal circuitry is advantageous to monitor spatiotemporal events of cerebellar development, in particular, PC development, which is essentially normal. More important, the lack of persistent multiple CFs input on developmentally challenged *Rora*$^{sg/sg}$ PCs provides a unique opportunity to analyze the postnatal maturation of the other excitatory afferents, the PFs in the *staggerer* mutant.

MATERIALS AND METHODS

Animals

The *staggerer* mutant is maintained on a C57BL/6J genetic background in the breeding colony at the animal facilities of the University of Groningen following the guidelines of the European Communities Council Directive of November 24, 1986 (86/609/EEC). Approval to conduct the study was obtained from the Ethics Committee on Animal Experimentation, University of Groningen (D4630C/D4285D). Homozygous *staggerer* (*Rora*$^{sg/sg}$), heterozygous *staggerer* (*Rora*$^{+/sg}$), and wildtype (*Rora*$^{+/+}$) mice were bred from *Rora*$^{+/sg}$ pairs. Animals had access to food and water ad libitum and were housed under controlled temperature (22 ± 2°C) and a 14/10-hour light/dark cycle.

In the litters, *Rora*$^{sg/sg}$, *Rora*$^{+/sg}$, and *Rora*$^{+/+}$ mice are generated in a 1:2:1 ratio. Since the latter two genotypes have indistinguishable traits, genotype analysis was required to differentiate *Rora*$^{+/+}$ *and Rora*$^{+/sg}$ animals. Genotype was determined a posteriori by polymerase chain reaction (PCR) on tail biopsy. The minimum number of animals required to show an effect was used, and procedures were designed to reduce or completely eliminate pain and distress. P0 animals were used. No apparent differences were found between *Rora*$^{+/sg}$ and *Rora*$^{+/+}$ pups and they were therefore considered as one group, referred to as control.

Genotype analysis

Genomic DNA was extracted from tail biopsies and amplified in two sets of reactions, one for each allele by PCR. *Staggerer* allele primers were: 5′-CGTTTGGCAAACTCCACC-3′ and 5′-GATTGAAAGCTGACTCGTTCC-3′. The + allele primers were: 5′-TCTCCCTTCTCAGTCCTGACA-3′ and 5′-TATATTCCACCACACGGCAA-3′. The amplified fragments (318 bp *Rora*$^{+}$ and 450 bp *Rora*^{sg}) were detected by electrophoresis on a 2% agarose gel.

Organotypic slice cultures of mouse cerebellum

Organotypic cerebellar cultures were prepared as previously described by Ghoumari et al. (2000). Briefly, brains were dissected into cold Gey's balanced salt solution (GBSS, Sigma, St. Louis, MO) supplemented with 5 mg/mL glucose and the meninges were removed. Parasagittal slices (350-μm thick) were cut on a McIlwain tissue chopper and transferred onto membranes of 30 mm Millipore membrane culture insert with 0.4 μm pore size (Millicell CM, Millipore, Bedford, MA). Slices were maintained in culture in six-well plates containing 1 mL/well of medium containing 50% basal medium with Earle's salts (BME; Invitrogen, La Jolla, CA), 2.5% Hank's balanced salt solution (HBSS; Invitrogen), 25% horse serum (Invitrogen), 1 mM L-glutamine, and 5 mg/mL glucose at 35°C in a humidified atmosphere with 5% CO_2. Medium was changed every 2–3 days.

Antibodies

1) Mouse monoclonal anti-calbindin D-28K (CaBP) (1:5,000 dilution; Cat. No. 300; Lot No. 18(F); Swant, Bellinzona, Switzerland) was raised in mouse against calbindin D-28K purified from chicken gut. It specifically stains the Ca^{++}-binding spot of calbindin D-28k (molecular weight 28 kD) in a two-dimensional gel and does not crossreact with calretinin or other known calcium-binding proteins (manufacturer's technical information). CaBP immunostaining is commonly used to study PCs, since in the cerebellar cortex it is specifically and strongly expressed in PCs (Celio et al., 1990).

2) Rabbit polyclonal anti-VGluT1 (1:1,000 dilution; Cat. No. 135302; Lot No. 2; Synaptic Systems, Germany) was generated in rabbits against a Strep-Tag fusion protein of rat VGLUT 1 (aa 456–560). The Strep-Tag fusion protein (aa 456–560 of rat VGLUT 1) has been tested in preadsorption experiments and blocks efficiently and specifically the corresponding signal in Western blots (manufacturer's technical information) and in immunolabeling (Zhou et al., 2007). VGLUT expression in the cerebellar cortex has been well documented (Takamori et al., 2001; Kaneko and Fujiyama, 2002; Hioki et al., 2003; Miyazaki et al., 2003; Hallberg et al., 2006). Our results were in agreement with previous studies on its distribution in the cerebellar cortex.

3) Guinea pig polyclonal anti-VGluT2 (1:1,000, kind gift from Prof. Watanabe, Hokkaido University School of Medicine, Japan). The affinity-purified polyclonal antibody to VGluT2 was generated in the guinea pig using C-terminus polypeptide–glutathione-S-transferase (GST) fusion proteins. The sequence of antigen polypeptides was 519–582 amino acid residues of rat VGluT2 (GenBank Access. No. AF271235). In the developing mouse cerebellum, specificity of the VGluT2 antibody, used in this study, and the VGluT1 antibody were assessed by Miyazaki et al. (2003) by means of immunoblotting, recognizing a 60-kDa protein band, and abolition of specific immunolabeling after preabsorption with antigen proteins. Miyazaki et al. (2003) showed further specificity and efficacy of the VGluT2 antibody in the developing mouse cerebellum by the use of immunoperoxidase, immunofluorescence and immunoelectron microscopy. Together, these results are consistent with immunostaining patterns in other studies using separate VGluT1 and VGluT2 antibodies (Takamori et al., 2000; Fremeau et al., 2001, 2004; Herzog et al., 2001).

4) Rabbit polyclonal anti-Pax-6 IgG (1:100 dilution; Cat. No. ab5790; Lot No. 0506001181; Chemicon, Temecula, CA) was used to visualize granule cells in the organotypic slices, since the protein is an external germinal layer marker and Pax-6 has been recognized as a critical regulator in cell polarization in the cerebellar granular cell (Yamasaki et al., 2001). The polyclonal Pax-6 IgG was raised in rabbit using a synthetic peptide: C-REEKLRNQRRQASNTPSHI, corresponding to amino acids 267–285 of Mouse Pax-6 (peptide available as ab5895, Abcam, Cambridge, MA). Specificity of the Pax-6 antibody used in this study was assessed by means of immunoblotting, recognizing a 47-kDa protein band (manufacturer's technical information).

5) Rabbit anti-mGluR1a antibodies (1:1,000 dilution; Cat. No. G9665; Lot No. 032K 1309; Sigma-Aldrich). The anti-glutamate receptor 1A, metabotropic antibody is produced in rabbit, synonyms: MDL number MFD01633637, MDL number: MFCD01633637. The immunogen is a synthetic peptide corresponding to the sequence of amino acid 1116–1130 of rat metabotropic glutamate receptor 1A (mGluR1a), with N-appended lysine, coupled to thyroglobulin using glutaraldehyde. The antibody is purified using peptide-agarose. It recognizes mGluR1a by immunoblotting and immunohistochemistry in tissues and cells from rat, mouse, and cat. The antibody does not react with other splice variants or mGluR5. The antibody was purchased from Sigma. The mGluR1A is abundant in PCs and is localized at the perijunctional site of both the PF-PC and CF-PC synapses (Baude et al., 1993; Nusser et al., 1994); this is in agreement with our observations.

6) Rabbit polyclonal anti-δ2 glutamate receptor (GluRδ2; 1:200 dilution; a kind gift from Prof. M. Watanabe, Hokkaido University School of Medicine, Japan) (Araki et al., 1993). Anti-GluRδ2 antibody was generated in rabbit using GST fusion protein containing the c-terminal of the δ2 subunit. The sequence of antigen polypeptides was 837–916 amino acid residues of the δ2 subunit of mouse. We have previously shown that the GluRδ2 antibody recognized a single band at $\approx$116 kDa in lysates both from normal cerebellum and from cerebellar organotypic slices (Gounko et al., 2005). Specific expression of this rabbit polyclonal anti-δ2 glutamate receptor in mouse and rat cerebellar Purkinje cells has been demonstrated by RNA blot, in situ hybridization analyses, immunoblotting, immunohistochemical, and electron microscope immunocytochemical analyses (Araki et al., 1993; Miyagi et al., 2002; Gounko et al., 2005).

Immunocytochemistry procedures

Cerebellar slices were fixed in 4% paraformaldehyde (PFA) in 0.1 M phosphate-buffer (PB) (pH 7.4) for 1 hour at room temperature.

Triple immunofluorescent labeling of CaBP, VGluT1, and VGluT2. After washing in PBS 0.1 M, slices were incubated for 1 hour in PBS containing 0.25% Triton X-100, 0.1% gelatin, and 0.1 M lysine. Slices were incubated with primary antibodies, mouse anti-calbindin D-28K (1:5,000), rabbit anti-VGluT1 (1:1000), and guinea pig anti-VGluT2 (1:1,000) overnight in PBS containing 0.25% Triton X-100 and 0.1% gelatin at 4°C. The following day, slices were washed and incubated for 2 hours with, respectively, Alexa-488 antimouse (1:200, Molecular Probes, Eugene, OR), Cy3-conjugated donkey antiguinea pig (1:500 dilution; Jackson Immunoresearch Laboratories, West Grove, PA), and Cy5-conjugated donkey antirabbit (1:500 dilution). Finally, slices were rinsed, mounted, and coverslipped in mowiol (Calbiochem, France Biochem, Meudon, France).

Immunofluorescent labeling of Pax-6. Slices were incubated with primary antibody, rabbit anti-Pax-6 (1:100) as described above. The following day, slices were washed and incubated for 2 hours with Alexa-488-conjugated donkey antirabbit (1:200 dilution; Molecular Probes). Slices were then rinsed, mounted, and coverslipped in mowiol.

Double immunofluorescent labeling of CaBP and mGluR1. Slices were incubated with primary antibodies, mouse anti-CaBP (1:5,000) and rabbit anti-mGluR1 (1:1000) as above. The following day, slices were washed and incubated for 2 hours with, respectively, Cy3-conjugated donkey antimouse (1:500 dilution; Jackson Immunoresearch Laboratories), and Alexa-488-conjugated donkey antirabbit (1:200 dilution; Molecular Probes). Slices were then rinsed, mounted, and coverslipped in mowiol.

Double immunofluorescent labeling of CaBP and GluRδ2. After 4% PFA fixation, slices were treated at 37°C for 1 minute with pepsin (Dako, Carpinteria, CA) in 0.2 N HCl. Slices were permeabilized and nonspecific binding blocked with 0.25% Triton X-100, 1% bovine serum albumin (BSA) (Sigma). Slices were incubated with primary antibodies, mouse anti-CaBP (1:5,000 dilution) and rabbit anti-GluRδ2 (1:200 dilution) at 4°C overnight. Primary antibodies were detected with Cy3-conjugated donkey antimouse (1:500 dilution; Jackson Immunoresearch Laboratories), and Alexa-488-conjugated donkey antirabbit IgG (1:200 dilution; Molecular Probes). After this, slices were rinsed, mounted, and coverslipped in mowiol.

Immunofluorescent images were captured with a confocal laser scanning microscope (Leica DMXR with confocal TCS NT unit; Germany) using 20× or 63× immersion lenses. Confocal images were acquired as a series of optical z-sections at 0.5-μm intervals through the whole PC. In double- and triple-labeling experiments, fluorescence was recorded separately. Images of individual optical sections were digitally stored for quantitative analysis.

Morphological analysis

To get a representative view of VGluT1 and VGluT2 immunoreactivity on individual PCs, we quantified the immunoreactive elements contacting the PCs. Series of optical z-sections of complete triple-labeled PCs were recorded successively for CaBP, VGluT1, and VGluT2 immunofluorescence. We used an ImageJ (NIH, Bethesda, MD)-macro to determine the area occupied by VGluT1 and VGluT2 terminals associated with the PC area in at least four different slices per group. In total, 311 PCs were analyzed and measurements were performed twice.

In control and *Rora*$^{sg/sg}$ organotypic slice cultures we measured the ratio of PC-associated VGluT1 and VGluT2 areas, and the ratio of the cellular distribution (soma vs. dendrites) of VGluT1- and VGluT2-positive terminals. The cultures were kept either for 7, 14, or 21 DIV. Furthermore, it was possible to estimate, for each genotype, the amount of VGluT1 and VGluT2 immunoreactive elements related to the PC surface. The postsynaptic distribution of mGluR1 and GluRδ2 has been qualitatively assessed. Figures were prepared using Adobe Photoshop v. 6.0 Software and Adobe Illustrator CS (Adobe System, San Jose, CA) to adjust contrast and brightness.

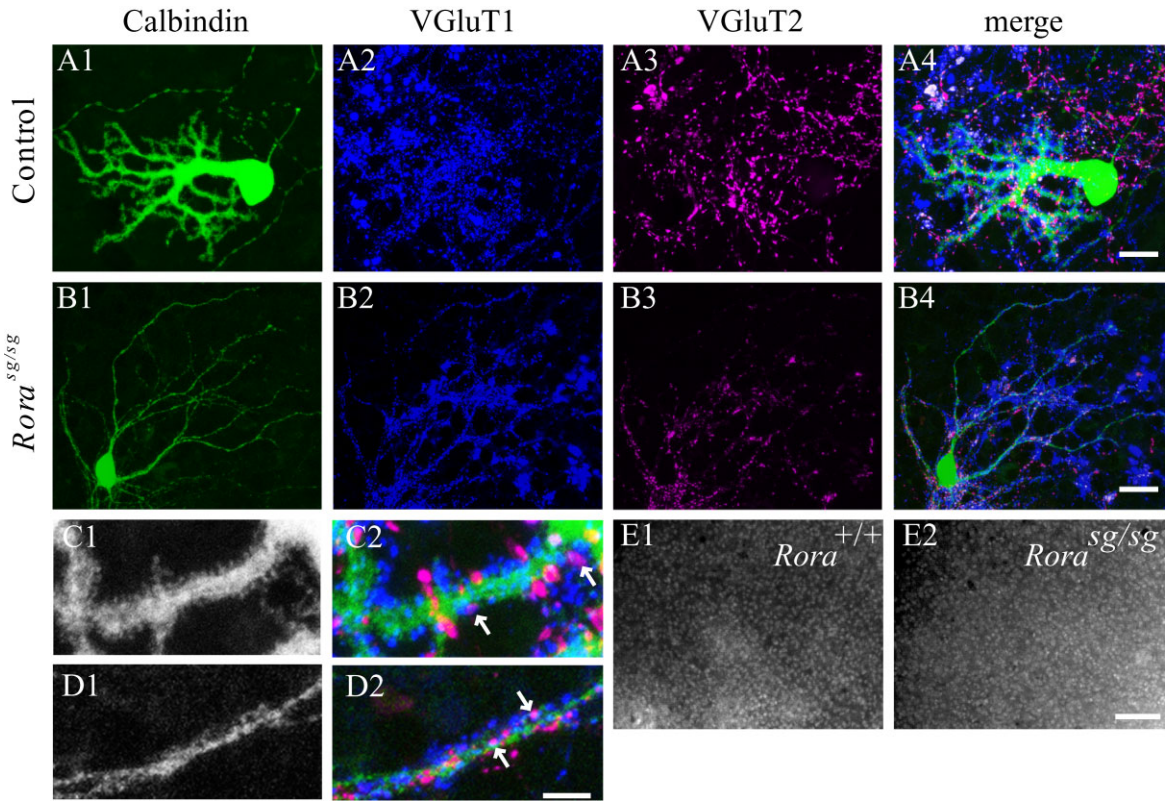

Figure 1.
Localization of VGluT1 and VGluT2 on PCs in P0–DIV21 organotypic cerebellar cultures of control (*Rora*$^{+/+}$ *and Rora*$^{+/sg}$) **(A,C)** or *Rora*$^{sg/sg}$ **(B,D)** mice. Triple immunofluorescence for CaBP (green) VGluT1 (blue) and VGluT2 (magenta). At this stage, control PCs are fully differentiated (A1), while the *Rora*$^{sg/sg}$ PC morphology still resembles a developmental stage observed at around birth (B1). PF terminals invade CF restricted areas along primary and secondary dendrites (see merged image A4 and B4). C,D: High-magnification view of dendrites is shown with presynaptic VGluT1- (blue) and VGluT2 (magenta)-positive terminals. In control slices, dendritic spines are associated with VGluT1 and 2 PFs (C1-2), whereas in *Rora*$^{sg/sg}$ slices VGluT1 and 2 PFs are also closely associated with dendrites lacking spines (D1-2). The distribution of granule cells in a control (E1) and *Rora*$^{sg/sg}$ (E2) cerebellar slice is revealed by PAX-6 staining **(E)**. Scale bars = 25 μm in A,B; 5 μm in C,D; 75 μm in E. [Color figure can be viewed in the online issue, which is available at www.interscience.wiley.com.]

Statistics

The mean area occupied by VGluT1 and VGluT2 terminals associated with the PC area were assessed by a two-way (age, genotype) analysis of variance (ANOVA) with, in case of interactions between genotype and age, multiple comparison of different groups by a Scheffé test. The ratios of VGluT1/VGlut2 immunolabeling per PC were assessed by one-way ANOVAs. Data are presented as the mean ± SEM.

RESULTS

Distribution of VGluT1 and VgluT2 terminals in P0-DIV21 slices

Figure 1 illustrates the triple immunohistochemical staining for CaBP, VGluT1, and VGluT2 of cerebellar slices of P0 control and *Rora*$^{sg/sg}$ pups kept for 21 DIV. At this stage, control PCs were fully differentiated (Fig. 1A1) while the *Rora*$^{sg/sg}$ PC morphology still resembled a developmental stage observed around birth (Armengol and Sotelo, 1991) (Fig. 1B1).

In both genotypes, VGluT1 and VGluT2 terminals were dense around PC, with more VGluT1 than VGluT2 terminals. VGluT1 and VGluT2 immunoreactivity appeared in beaded or varicose fibers and as coarse VGluT1 and VGluT2 immunodeposits (Fig. 1A2–A4,B2–B4). VGluT1 and VGluT2 were not evenly distributed in P0 slices, although this was not related to the distribution of granule cells as revealed by Pax-6 staining (Fig. 1E). Furthermore, the absence of CFs resulted in an invasion of VGluT1- and VGluT2-positive PFs on proximal dendrites and even the soma of PCs (Fig. 1A,B). In some rare cases VGluT1 and VGluT2 immunoreactivity could be detected around PC axons (Fig. 1A).

There were genotype differences in the distribution of VGluT1 and VGluT2 terminals on PCs. On control PCs, VGluT1- and VGluT2-positive puncta were localized on proximal dendrites and closely associated with spines (Fig. 1C). Some terminal-like structures apposed to PCs showed immunoreactivity for both transporters (Fig. 1C2,D2). On *Rora*$^{sg/sg}$ PCs, which lack tertiary dendrites and are spineless (Fig. 1B,D), VGluT1 and VGluT2 puncta were apposed to the soma and primary and secondary dendrites (Figs. 1B,D, 2).

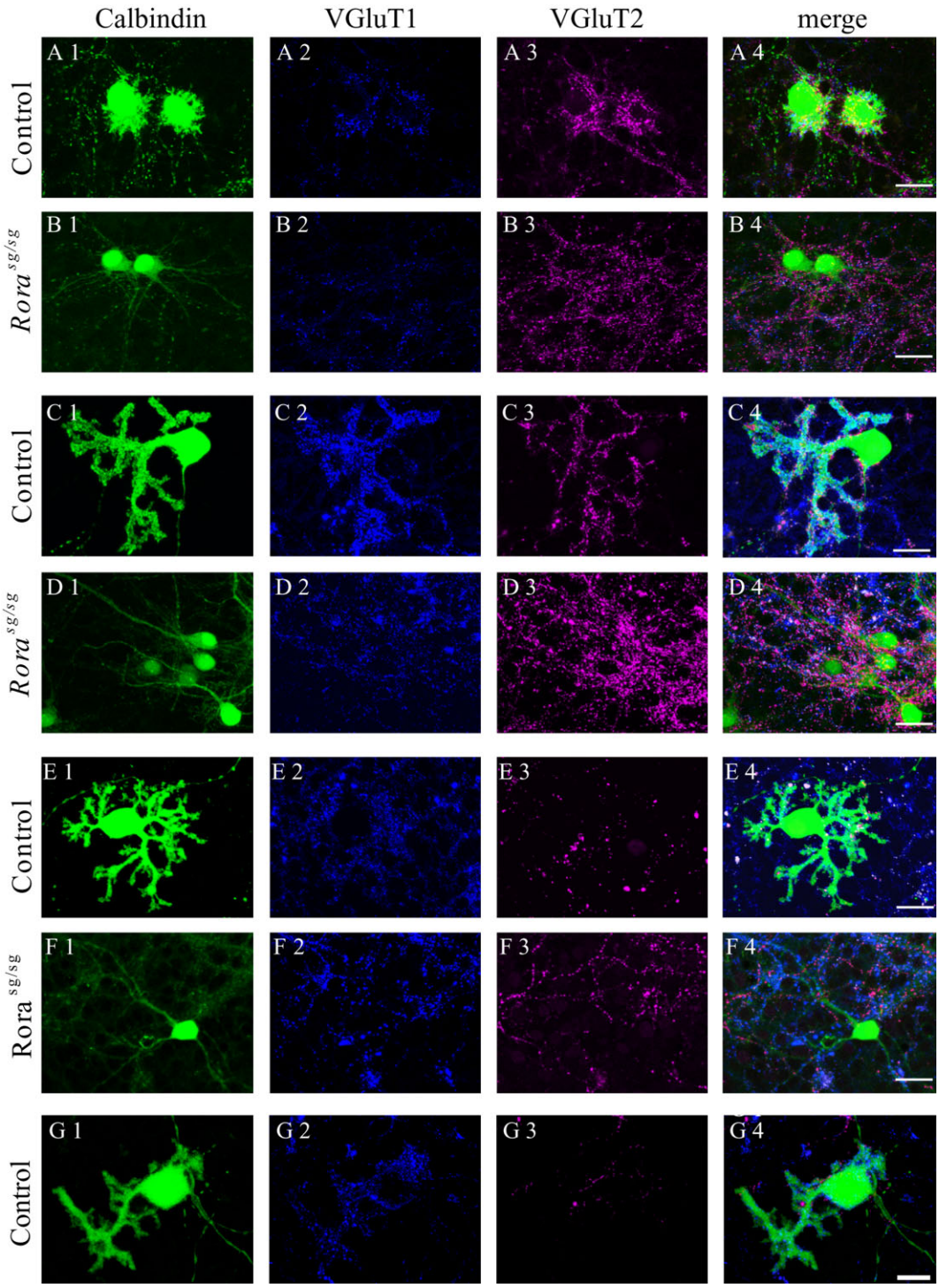

Figure 2.
VGluT2-to-VGluT1 switch is delayed in the *Rora*$^{sg/sg}$ mutant. Organotypic cultures from control (*Rora*$^{+/+}$ *and Rora*$^{+/sg}$) **(A,C,E,G)** or *Rora*$^{sg/sg}$ or **(B,D,F)** P0 mice after 7 DIV (A,B), 14 DIV (C,D), 21 DIV (E,F), and 28 DIV (G). Triple immunofluorescence for CaBP (green) VGluT1 (blue) and VGluT2 (magenta). During postnatal development *Rora*$^{sg/sg}$ PCs remained fusiform, however, prolonging their simple dendrites (B1,D1,F1); control PCs differentiated into cells with an extensive and complex dendritic tree (A1,C1,E1). In control slices, VGluT1 immunolabeling was increased until 14 DIV with a concomitant decrease in VGluT2 immunolabeling (A4,C4,E4), whereas in *Rora*$^{sg/sg}$ slices VGluT1 immunolabeling increased until 21 DIV, and VGluT2 immunolabeling decreased after 14 DIV. Note the intense concentration of VGluT2 immunolabeling around the PC soma and the short protrusions of *Rora*$^{sg/sg}$ PCs after 14 DIV (D4 and Fig. 4). Some control PCs were contacted by VGluT2 terminals even after 28 DIV (G3,G4). Scale bars = 25 μm. [Color figure can be viewed in the online issue, which is available at www.interscience.wiley.com.]

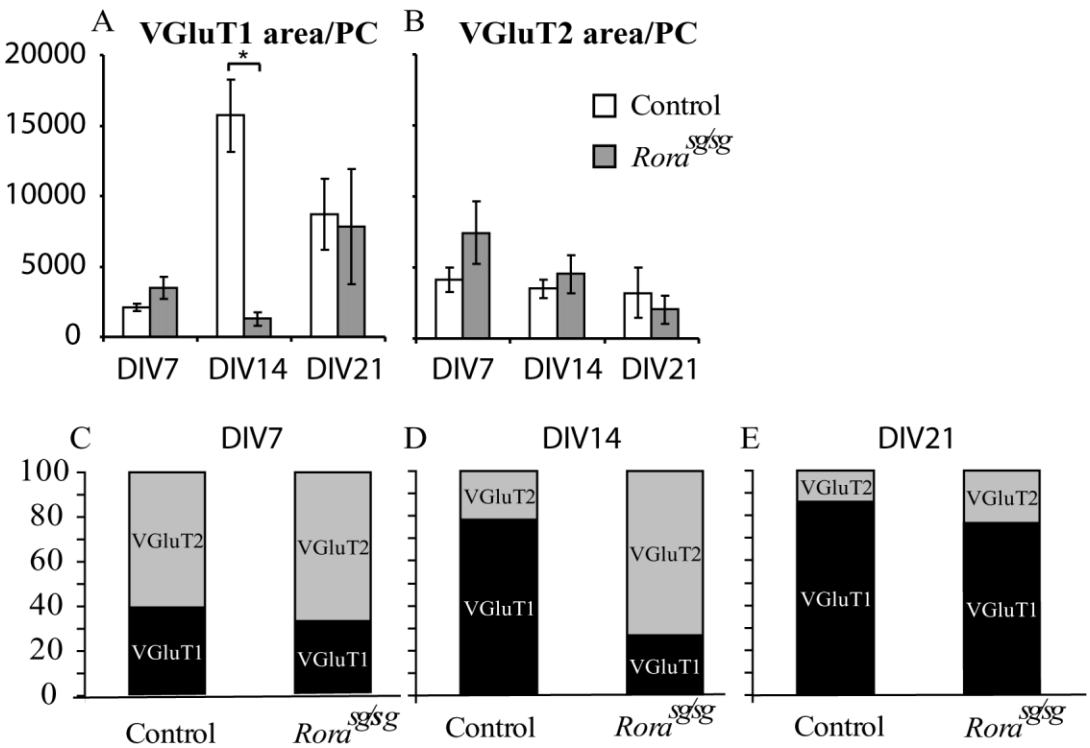

Figure 3.
Quantitative analysis of VGluT2 and VGluT 1 terminals contacting normal and *Rora*$^{sg/sg}$ PCs between P0–DIV7 and P0–DIV21. Top panels: Quantitative analysis of VGluT2 and VGluT1 area per Purkinje cell. The area is expressed in pixels. After DIV14 VGluT1 labeling was more intense around control than *Rora*$^{sg/sg}$ PCs **(A)**. No significant differences were observed in VGluT2 expression according to age or genotype **(B)**. Data in A,B are presented as the mean ± SEM. *$P < 0.001$. Bottom panels: comparisons of VGLuT1/VGluT2 ratios. After 7 and 21 DIV no genotype differences were observed in VGluT2/VGluT1 ratios at PF-PC contact **(C,E)**. In contrast, in *Rora*$^{sg/sg}$ slices the VGluT2/VGluT1 ratio remained similar after 7 and 14 DIV **(C,D)** with more VGluT2 than VGluT1 terminals, whereas PFs in control slices mainly expressed VGluT1 at 14DIV and thereafter (D,E).

VGluT2-to-VGluT1 switching in PFs is delayed in *staggerer* ex vivo

Next we examined the spatiotemporal distribution of VGluT1 and VGluT2 terminals in PF varicosities contacting developing PCs (Fig. 2). Ex vivo the distribution of VGluT1 and VGluT2 in PF terminals underwent remarkable changes during the first 3 weeks of postnatal development. In agreement with previous studies in vivo (Miyazaki et al., 2003) we found globally increasing densities of VGluT1-positive terminals throughout postnatal development, with a peak after 14 DIV in controls slices, when the density is 90% higher than in *Rora*$^{sg/sg}$ slices ($P < 0.001$; Fig. 3A). No differences in densities of VGluT2-positive terminals were found according to age or genotype in slices after 7, 14, or 21 DIV (Fig. 3B).

However, the comparison of the ratio of VGluT1/VGluT2 PF terminals at ages P0–DIV7, P0–DIV14, and P0–DIV21 revealed a different timing of the VGluT2-to-VGluT1 switching in *Rora*$^{sg/sg}$ and control slices (Figs. 2, 3). After 7 DIV, the percentage of VGluT1 and VGluT2 terminals contacting control PCs were, respectively, 40% and 60%, and contacting *Rora*$^{sg/sg}$ PC 34% and 66% (Figs. 2A,B, 3C). One week later, at P0–DIV14, the proportion of VGluT1 terminals contacting control PCs had doubled (78%) and VGluT2 expression had diminished (22%; Figs. 2C, 3D). In contrast, the ratio of VGluT1/VGluT2 terminals contacting *Rora*$^{sg/sg}$ PCs remained stable until DIV14 (27/73) (Fig. 2D and 3D). At P0–DIV21 the difference between the genotypes had disappeared (Figs. 2E,F, 3E). At this stage the ratio of VGluT1/VGluT2-labeled terminals contacting control PCs was 86/14 while, the ratio of VGluT1/VGluT2 contacting *Rora*$^{sg/sg}$ PC was 77/33 (Fig. 3E). Interestingly, even at the later stages studied (P0–DIV28 and P0–DIV42) some PF terminals contacting PCs remain VGluT2-positive (Fig. 2G).

VGluT2 accumulation around *Rora*$^{sg/sg}$ Purkinje cells

In contrast to control PCs, there was a strong accumulation of VGluT2-positive terminals around *Rora*$^{sg/sg}$ PC somatic areas and proximal primary dendrites, particularly after 14 DIV (Fig. 4A,B). To address the question of whether, ex vivo, in the absence of excitatory CF inputs, PF terminals contact PC areas normally innervated by CFs in vivo were preferentially VGluT1- or VGluT2-positive, we measured in the same series of control P0–14 DIV slices the ratio of VGluT1/VGluT2 terminals both on PC soma and dendrites. After 14 DIV the proportion of VGlut2 terminals was not significantly higher on PC soma than on PC dendrites, respectively 39% versus 19% (Fig. 4C). The multiple short protrusions from *Rora*$^{sg/sg}$ PC soma, the decreased numbers of secondary dendrites, and

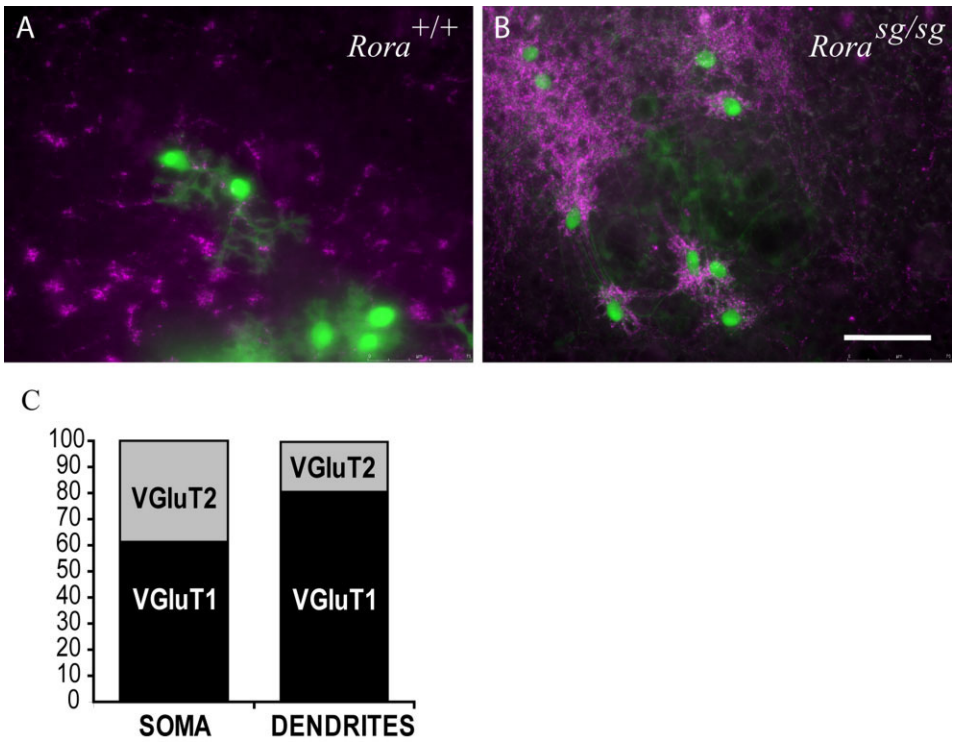

Figure 4.
VGluT2 accumulations around *Rora*$^{sg/sg}$ PCs in organotypic cultures slices from control **(A)** or *Rora*$^{sg/sg}$ **(B)** P0 mice after 14 DIV. Double immunofluorescence for CaBP (green) and VGluT2 (magenta). After 14 DIV, VGluT2 immunolabeling was decreased in control animals (A), whereas it remained intense in *Rora*$^{sg/sg}$ slices. Note the concentration of VGluT2 immunolabeling around the PC soma and the short protrusions of *Rora*$^{sg/sg}$ PCs. Quantitative analysis of VGLuT1/VGluT2 ratios on the dendritic tree vs. soma and proximal dendrites in normal PCs after 14 DIV **(C)**. NB: These ratios were similar on soma or dendrites (C). The immature morphology of *Rora*$^{sg/sg}$ PCs made this analysis unreliable on mutant slices. Scale bar = 75 μm in B (applies to A). [Color figure can be viewed in the online issue, which is available at www.interscience.wiley.com.]

the lack of tertiary dendrites made it impossible to perform a similarly reliable analysis in *Rora*$^{sg/sg}$ slices.

We next correlated VGluT immunoreactivity patterns with staining patterns of the glutamatergic receptors mGluR1 and GluRδ2, which in vivo are expressed specifically at postsynaptic PF-PC contacts.

Diminished mGluR1 immunoreactivity in *Rora*$^{sg/sg}$ PCs ex vivo

Figure 5 shows P0 DIV14 and P0 DIV control and *Rora*$^{sg/sg}$ slices labeled with anti-mGluR1 receptors. After 14 DIV, control PCs (Fig. 5A) showed intense mGluR1 labeling in dendritic tree and soma, and weaker labeling in a subpopulation of granule cells and few other neurons, possibly Golgi cells. Stellate and basket cells were not discernable. After 21 DIV, mGluR1 labeling remained intense in the dendritic area of PCs, localized to spines, and was only light in the soma (Fig. 5C). Axonal projections lacked mGluR1 labeling either after 14- or 21-DIV.

In contrast, the staining pattern for mGluR1 receptors was different in *Rora*$^{sg/sg}$ slices. Immunolabeling for mGluR1 of *Rora*$^{sg/sg}$ PCs was weak, particularly after 14 DIV (Fig. 5B2,B3) and showed a punctate distribution. Other cells in the slice displayed a moderate immunoreactivity for mGluR1. Note that mGluR1 appears at the margin of the dendritic shafts of *Rora*$^{sg/sg}$ PCs, although no spines are present (Fig. 5D).

Somatic GluRδ2 protein accumulation in *Rora*$^{sg/sg}$ PCs in long-term cultured slices

At P0–DIV14, GluRδ2 immunoreactivity was present both in somatic and dendritic areas of control PCs, whereas no reliable immunoreactivity was detected in *Rora*$^{sg/sg}$ PCs (Fig. 6A,B). At P0–DIV21, control PCs showed an intense GluRδ2 immunolabeling along the dendritic branches, especially in the dendritic spines (Fig. 6C). A weak immunolabeling was still noted in the PC soma (Fig. 6C2).

At the same stage, the staining pattern for GluRδ2 receptors was different in *Rora*$^{sg/sg}$ PCs (Fig. 6D). To our knowledge this is the first time that the GluRδ2 protein has been detected in *Rora*$^{sg/sg}$ PCs. After 21 DIV there was strong GluRδ2 immunolabeling at *Rora*$^{sg/sg}$ PC soma, with few GluRδ2 labels in primary dendrites. In the soma, GluRδ2 immunolabeling was specifically intense in the apical side of the *Rora*$^{sg/sg}$ PC soma (Fig. 6D). The staining pattern for GluRδ2 and mGluR1 receptors clearly differed in intensity and distribution, the mGluR1 labeling being weaker and more uniformly distributed (Figs. 5D2, 6D2).

DISCUSSION

By using cerebellar cultures from wildtype and *Rora*$^{+/sg}$ P0 mice we show that granule cells recapitulate ex vivo the devel-

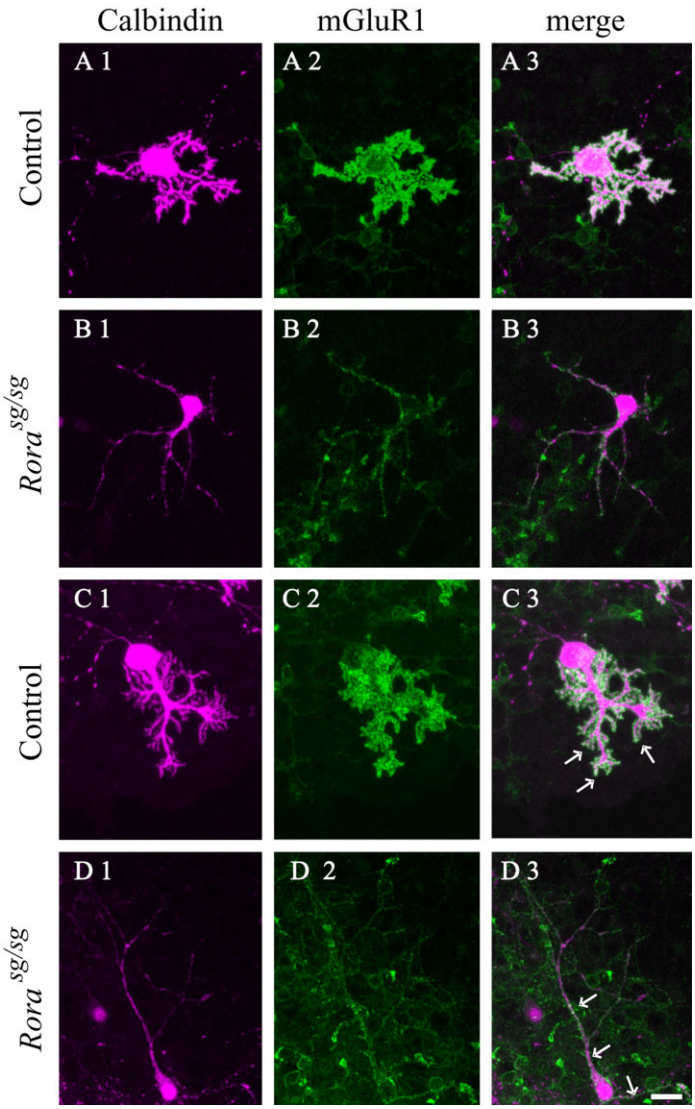

Figure 5.
Localization of mGluR1 in P0 control **(A,C)** and *Rora*$^{sg/sg}$ **(B,D)** PCs in organotypic cerebellar cultures kept for 14 and 21 DIV. Representative images of double immunofluorescence for CaBP (magenta) and mGluR1 (green) after DIV14 (A,B) and DIV21 (C,D). In control PCs, strong mGluR1 immunolabeling was noticeable in PC dendrites and weaker immunolabeling in the soma after 14 and 21 DIV (A2 and C2). Arrows point to mGluR1 immunolabeling on control PC spines after 21 DIV. In contrast, mGluR1 immunoreactivity was greatly reduced in *Rora*$^{sg/sg}$ PCs and appeared evenly distributed in soma and dendrites at both ages studied (14 and 21DIV). Scale bar = 25 μm. [Color figure can be viewed in the online issue, which is available at www.interscience.wiley.com.]

opmental expression of VGluT1 and VGluT2 in PF terminals described in vivo (Miyazaki et al., 2003) and in rat granule cell cultures in vitro (Hallberg et al., 2006). We also found that ex vivo, as in early studies in vivo (Sotelo and Arsenio-Nunes, 1976), the absence of CFs leads to the extension of PF terminals onto the primary dendrites and soma of control PCs. In *Rora*$^{sg/sg}$ cerebellar slices this appeared more evident, since VGluT1- and VGluT2-positive PF terminals accumulated around the *Rora*$^{sg/sg}$ PC soma and proximal primary dendrites. The different distribution of VGluT1 and VGluT2 terminals on control or *Rora*$^{sg/sg}$ PCs was unlikely due to the massive death of *Rora*$^{sg/sg}$ PCs, as observed in vivo, since in organotypic slice culture *Rora*$^{sg/sg}$ PCs have higher survival rates (Boukhtouche et al., 2006b). Ex vivo, *Rora*$^{sg/sg}$ PCs grow progressively longer dendrites but are unable to progress beyond an early fusiform stage of differentiation (Shirley and Messer, 2004; Boukhtouche et al., 2006b). In vivo, *Rora*$^{sg/sg}$ PCs develops synapses with CFs, but their dendritic tree might be too immature and not provide enough space for sufficient PF innervation. Since in the present study we showed that in cerebellar cultures PFs did contact the long and thin spineless *Rora*$^{sg/sg}$ dendrites, we therefore suggest that it is the poor dendritic development of *Rora*$^{sg/sg}$ PC in vivo that drives PFs to expand their territory to include the *Rora*$^{sg/sg}$ PC soma.

In vivo during postnatal cerebellar development, from P10 onward, VGluT1 gradually replaces VGluT2 in PF terminals in a spatiotemporal pattern, with VGluT1 expression

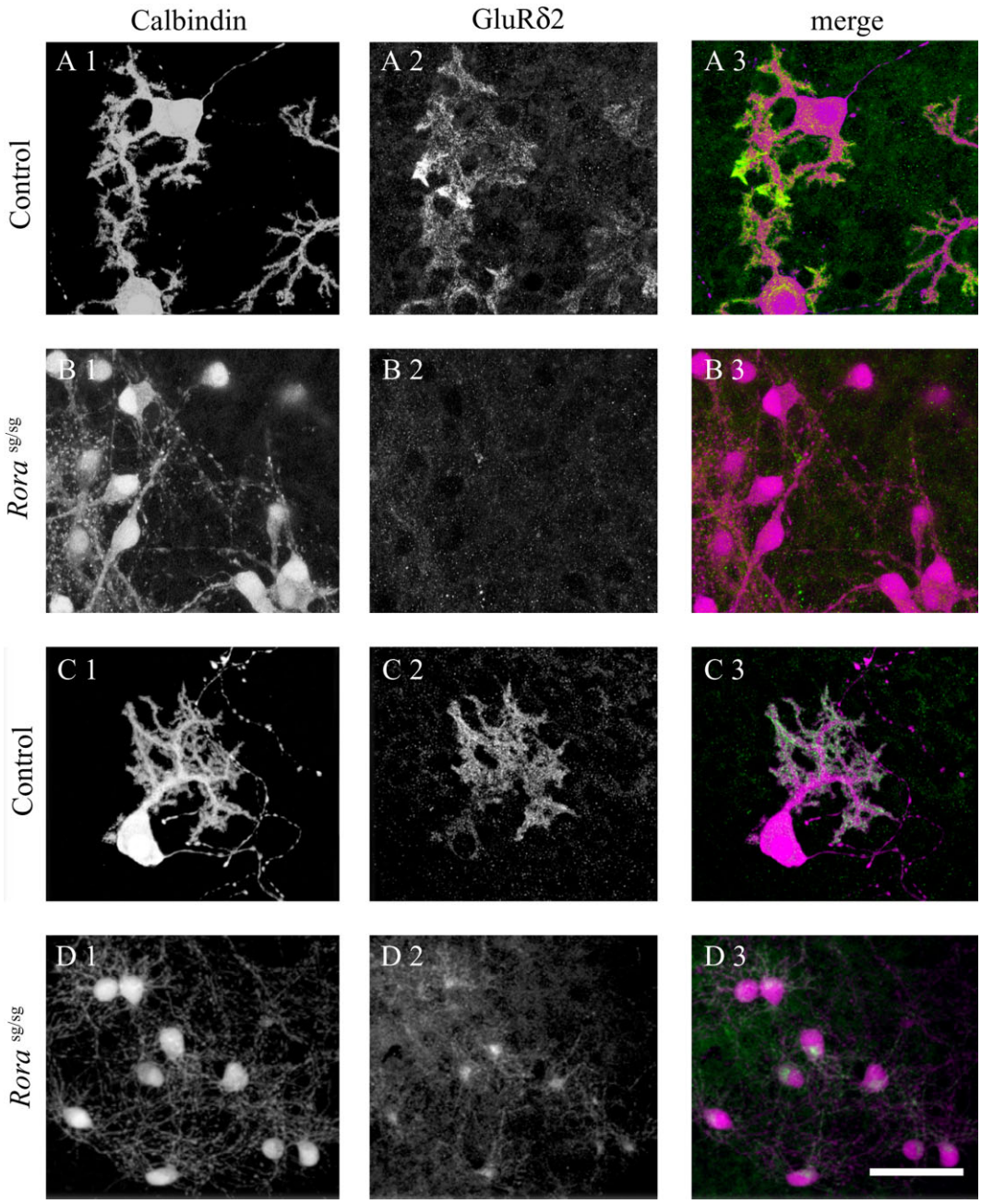

Figure 6.
Perisomatic GluRδ2 accumulation in P0 *Rora*$^{sg/sg}$ PCs kept for 21 DIV. Double immunofluorescence for CaBP (magenta) and GluRδ2 (green). After 14 DIV GluRδ2 was expressed in control PCs both in soma and dendrites **(A)**, but no reliable GluRδ2 could be detected in *Rora*$^{sg/sg}$ PCs. After 21 DIV, as shown in the merged image **(C3,D3)**, GluRδ2 was mainly localized in spines in control PCs. In contrast, GluRδ2 labeling was scarce in *Rora*$^{sg/sg}$ PC dendrites, but was accumulated in the somatic region of the *Rora*$^{sg/sg}$ PC (D2,D3). Scale bar = 50 μm. [Color figure can be viewed in the online issue, which is available at www.interscience.wiley.com.]

moving from internal (i.e., proximal dendrites) to external (i.e., distal dendrites) parts of the molecular layer and correlating with CF translocation (Miyazaki et al., 2003). However, in culture this laminar distribution of molecular, PC, and granule cell layer is mostly abolished, plus there is no CF innervation. Thus, after 14 DIV the higher proportion of VGluT2-positive PF terminals on control PC soma and proximal primary dendrites might indicate 1) different regulatory mechanisms at CF-PC synapses, compared to PF-PC connection sites, or 2) the simple lack of layered organization.

In the present study we provide evidence that the VGluT2-to-VGluT1 switch is delayed in PF terminals of *Rora*$^{sg/sg}$ granule cells, suggesting delayed granule cell

maturation. In the cerebellum, RORα is highly expressed in PCs, and to a lesser extent in a number of interneurons, but not in granule cells (Hamilton et al., 1996; Steinmayr et al., 1998; Ino, 2004). The failure of a proper PC-PF connection in *Rora*$^{sg/sg}$ PCs (Sotelo and Changeux 1974; Herrup and Mullen 1979) might slow down the maturation of PFs. A possible mechanism is via altered levels of neurotrophin expression and reduced transcription response to thyroid hormone in *Rora*$^{sg/sg}$ and *Rora*$^{-/-}$ mice (Koibuchi et al., 1999; Qiu et al., 2007).

To assess the degree of PF-PC synaptic maturation in *Rora*$^{sg/sg}$ PCs ex vivo, we also analyzed the expression pattern of two postsynaptic receptors, mGluR1 and GluRδ2. In vivo, in adult wildtype PCs, mGluR1 is present at both PF and CF synapses, whereas GluRδ2 is only found at PF synapses (Baude et al., 1993; Nusser et al., 1994; Takayama et al., 1996; Landsend et al., 1997; Lopez-Bendito et al., 2001). We found that ex vivo in *Rora*$^{sg/sg}$ PCs the immunoreactivity for mGluR1 receptors was weak and evenly distributed along the PC inner membrane. However, this did not match the presynaptic staining pattern of VGluT1 terminals, which were more intense on the PC soma, as shown in *Rora*$^{sg/sg}$ cerebellum in vivo (Ryo et al., 1993). Interestingly, PF-PC synapse formation appears normal in mGluR1 mutant mice (Kano et al., 1997), but does lead to persistent CF innervation. The *staggerer* mutant, on the other hand, displays low levels of mGLuR1, persistent CF innervation, but has a dysfunctional PF-PC synapse formation.

We found that in cerebellar slices, after 21 DIV immunoreactivity for GluRδ2 was more evident in the apical part of the soma of *Rora*$^{sg/sg}$ PCs than in its dendrites, where labeling was scarce. This contrasts to control PCs were that the GluRδ2 labeling was restricted to the dendrites, as is seen in vivo by 21 days. However, the accumulation in ex vivo *Rora*$^{sg/sg}$ PCs of somatic GluRδ2 appeared to be cytoplasmic rather than membrane-bound. In wildtype PCs, GluRδ2 is efficiently transported to the PC surface with only a few GluRδ2 proteins being retained in the cytoplasmic pool (Yuzaki, 2003). The fact that in *Rora*$^{sg/sg}$ PCs, GluRδ2 was found more in somatic areas compared to dendrites might be due to a defective intracellular trafficking of GluRδ2 proteins to dendritic areas and membranes. Previous studies on the double mutant *staggerer/lurcher* imply that the *staggerer* mutation blocks mutant receptor protein localization rather than mRNA transcription (Messer and Kang, 2000). We need to learn more about the intracellular trafficking of GluRδ2 in the immature dendrites of *Rora*$^{sg/sg}$ PCs. Indeed, adequate surface expression of GluRδ2 is essential to its role in the formation and/or maintenance of PF-PC synapses (Kurihara et al., 1997; Morando et al., 2001; Yuzaki, 2003), as is illustrated by GluRδ2$^{-/-}$ mutant mice, in which PF-PC synaptogenesis is impaired with up to 40% of PC being devoid of PF synapses (Kurihara et al., 1997).

Taken together, our data have linked defective RORα expression in PCs to a delayed differentiation of granule cells, as revealed by the delayed switch of the glutamate transporters VGluT2 into VGluT1 in the PF terminal, and to an altered distribution of the postsynaptic glutamate receptors mGluR1 and GluRδ2 in *Rora*$^{sg/sg}$ PCs. This enlightens a novel role of RORα in cerebellar circuitry formation.

ACKNOWLEDGMENTS

We thank F. Dijk for help with the immunocytochemistry and D. Huizinga and Dr. C. Salim for assistance with the image preparations. We thank Dr. R. Sherrard for constructive comments and help with the English.

LITERATURE CITED

Araki K, Meguro H, Kushiya E, Takayama C, Inoue Y, Mishina M. 1993. Selective expression of the glutamate receptor channel delta 2 subunit in cerebellar Purkinje cells. Biochem Biophys Res Commun 197:1267–1276.

Armengol JA, Sotelo C. 1991. Early dendritic development of Purkinje cells in the rat cerebellum. A light and electron microscopic study using axonal tracing in 'in vitro' slices. Brain Res Dev Brain Res 64:95–114.

Baude A, Nusser Z, Roberts JD, Mulvihill E, McIlhinney RA, Somogyi P. 1993. The metabotropic glutamate receptor (mGluR1 alpha) is concentrated at perisynaptic membrane of neuronal subpopulations as detected by immunogold reaction. Neuron 11:771–787.

Boukhtouche F, Doulazmi M, Frederic F, Dusart I, Brugg B, Mariani J. 2006a. RORalpha, a pivotal nuclear receptor for Purkinje neuron survival and differentiation: from development to ageing. Cerebellum 5:97–104.

Boukhtouche F, Janmaat S, Vodjdani G, Gautheron V, Mallet J, Dusart I, Mariani J. 2006b. Retinoid-related orphan receptor alpha controls the early steps of Purkinje cell dendritic differentiation. J Neurosci 26: 1531–1538.

Bradley P, Berry M. 1978. The Purkinje cell dendritic tree in mutant mouse cerebellum. A quantitative Golgi study of Weaver and Staggerer mice. Brain Res 142:135–141.

Celio MR, Baier W, Scharer L, Gregersen HJ, de Viragh PA, Norman AW. 1990. Monoclonal antibodies directed against the calcium binding protein Calbindin D-28k. Cell Calcium 11:599–602.

Chedotal A, Sotelo C. 1992. Early development of olivocerebellar projections in the fetal rat using CGRP immunocytochemistry. Eur J Neurosci 4:1159–1179.

Crepel F. 1982. Regression of functional synapses in the immature mammalian cerebellum. Trends Neurosci 5:266–269.

Crepel F, Mariani J, Delhaye-Bouchaud N. 1976. Evidence for a multiple innervation of Purkinje cells by climbing fibers in the immature rat cerebellum. J Neurobiol 7:567–578.

Crepel F, Delhaye-Bouchaud N, Guastavino JM, Sampaio I. 1980. Multiple innervation of cerebellar Purkinje cells by climbing fibres in staggerer mutant mouse. Nature 283:483–484.

Doulazmi M, Frederic F, Capone F, Becker-Andre M, Delhaye-Bouchaud N, Mariani J. 2001. A comparative study of Purkinje cells in two RORalpha gene mutant mice: staggerer and RORalpha(-/-). Brain Res Dev Brain Res 127:165–174.

Dusart I, Airaksinen MS, Sotelo C. 1997. Purkinje cell survival and axonal regeneration are age dependent: an in vitro study. J Neurosci 17:3710–3726.

Eccles JC, Llinas R, Sasaki K. 1966. The excitatory synaptic action of climbing fibres on the Purkinje cells of the cerebellum. J Physiol 182:268–296.

Fremeau RT Jr, Troyer MD, Pahner I, Nygaard GO, Tran CH, Reimer RJ, Bellocchio EE, Fortin D, Storm-Mathisen J, Edwards RH. 2001. The expression of vesicular glutamate transporters defines two classes of excitatory synapse. Neuron 31:247–260.

Fremeau RT Jr, Voglmaier S, Seal RP, Edwards RH. 2004. VGLUTs define subsets of excitatory neurons and suggest novel roles for glutamate. Trends Neurosci 27:98–103.

Gold DA, Baek SH, Schork NJ, Rose DW, Larsen DD, Sachs BD, Rosenfeld MG, Hamilton BA. 2003. RORalpha coordinates reciprocal signaling in cerebellar development through sonic hedgehog and calcium-dependent pathways. Neuron 40:1119–1131.

Gold DA, Gent PM, Hamilton BA. 2007. ROR alpha in genetic control of cerebellum development: 50 staggering years. Brain Res 1140:19–25.

Gounko NV, Rybakin V, Kalicharan D, Siskova Z, Gramsbergen A, van der Want JJ. 2005. CRF and urocortin differentially modulate GluRdelta2 expression and distribution in parallel fiber-Purkinje cell synapses. Mol Cell Neurosci 30:513–522.

Gounko NV, Gramsbergen A, van der Want JJ. 2007. The glutamate

receptor delta 2 in relation to cerebellar development and plasticity. Neurosci Biobehav Rev 31:1095–1100.

Hallberg OE, Bogen IL, Reistad T, Haug KH, Wright MS, Fonnum F, Walaas SI. 2006. Differential development of vesicular glutamate transporters in brain: an in vitro study of cerebellar granule cells. Neurochem Int 48:579–585.

Hamilton BA, Frankel WN, Kerrebrock AW, Hawkins TL, FitzHugh W, Kusumi K, Russell LB, Mueller KL, van Berkel V, Birren BW, Kruglyak L, Lander ES. 1996. Disruption of the nuclear hormone receptor RORalpha in staggerer mice. Nature 379:736–739.

Herrup K. 1983. Role of staggerer gene in determining cell number in cerebellar cortex. I. Granule cell death is an indirect consequence of staggerer gene action. Brain Res 313:267–274.

Herzog E, Bellenchi GC, Gras C, Bernard V, Ravassard P, Bedet C, Gasnier B, Giros B, El MS. 2001. The existence of a second vesicular glutamate transporter specifies subpopulations of glutamatergic neurons. J Neurosci 21:RC181.

Hioki H, Fujiyama F, Taki K, Tomioka R, Furuta T, Tamamaki N, Kaneko T. 2003. Differential distribution of vesicular glutamate transporters in the rat cerebellar cortex. Neuroscience 117:1–6.

Hirano T. 2006. Cerebellar regulation mechanisms learned from studies on GluRdelta2. Mol Neurobiol 33:1–16.

Ino H. 2004. Immunohistochemical characterization of the orphan nuclear receptor ROR alpha in the mouse nervous system. J Histochem Cytochem 52:311–323.

Ito M. 1989. Long-term depression. Annu Rev Neurosci 12:85–102.

Kaneko T, Fujiyama F. 2002. Complementary distribution of vesicular glutamate transporters in the central nervous system. Neurosci Res 42:243–250.

Kano M, Hashimoto K, Kurihara H, Watanabe M, Inoue Y, Aiba A, Tonegawa S. 1997. Persistent multiple climbing fiber innervation of cerebellar Purkinje cells in mice lacking mGluR1. Neuron 18:71–79.

Koibuchi N, Liu Y, Fukuda H, Takeshita A, Yen PM, Chin WW. 1999. ROR alpha augments thyroid hormone receptor-mediated transcriptional activation. Endocrinology 140:1356–1364.

Kurihara H, Hashimoto K, Kano M, Takayama C, Sakimura K, Mishina M, Inoue Y, Watanabe M. 1997. Impaired parallel fiber—>Purkinje cell synapse stabilization during cerebellar development of mutant mice lacking the glutamate receptor delta2 subunit. J Neurosci 17:9613–9623.

Landsend AS, miry-Moghaddam M, Matsubara A, Bergersen L, Usami S, Wenthold RJ, Ottersen OP. 1997. Differential localization of delta glutamate receptors in the rat cerebellum: coexpression with AMPA receptors in parallel fiber-spine synapses and absence from climbing fiber-spine synapses. J Neurosci 17:834–842.

Linden DJ, Connor JA. 1995. Long-term synaptic depression. Annu Rev Neurosci 18:319–357.

Lopez-Bendito G, Shigemoto R, Lujan R, Juiz JM. 2001. Developmental changes in the localisation of the mGluR1alpha subtype of metabotropic glutamate receptors in Purkinje cells. Neuroscience 105:413–429.

Mariani J. 1982. Extent of multiple innervation of Purkinje cells by climbing fibers in the olivocerebellar system of weaver, reeler, and staggerer mutant mice. J Neurobiol 13:119–126.

Mariani J, Changeux JP. 1980. Multiple innervation of Purkinje cells by climbing fibers in the cerebellum of the adult staggerer mutant mouse. J Neurobiol 11:41–50.

Mariani J, Changeux JP. 1981. Ontogenesis of olivocerebellar relationships. I. Studies by intracellular recordings of the multiple innervation of Purkinje cells by climbing fibers in the developing rat cerebellum. J Neurosci 1:696–702.

Messer A, Kang X. 2000. Control of transcription in the RORa-staggerer mutant mouse cerebellum: glutamate receptor delta2 mRNA. Int J Dev Neurosci 18:663–668.

Miyagi Y, Yamashita T, Fukaya M, Sonoda T, Okuno T, Yamada K, Watanabe M, Nagashima Y, Aoki I, Okuda K, Mishina M, Kawamoto S. 2002. Delphilin: a novel PDZ and formin homology domain-containing protein that synaptically colocalizes and interacts with glutamate receptor delta 2 subunit. J Neurosci 22:803–814.

Miyazaki T, Fukaya M, Shimizu H, Watanabe M. 2003. Subtype switching of vesicular glutamate transporters at parallel fibre-Purkinje cell synapses in developing mouse cerebellum. Eur J Neurosci 17:2563–2572.

Morando L, Cesa R, Rasetti R, Harvey R, Strata P. 2001. Role of glutamate delta-2 receptors in activity-dependent competition between heterologous afferent fibers. Proc Natl Acad Sci U S A 98:9954–9959.

Nusser Z, Mulvihill E, Streit P, Somogyi P. 1994. Subsynaptic segregation of metabotropic and ionotropic glutamate receptors as revealed by immunogold localization. Neuroscience 61:421–427.

Qiu CH, Shimokawa N, Iwasaki T, Parhar IS, Koibuchi N. 2007. Alteration of cerebellar neurotropin messenger ribonucleic acids and the lack of thyroid hormone receptor augmentation by staggerer-type retinoic acid receptor-related orphan receptor-alpha mutation. Endocrinology 148:1745–1753.

Ryo Y, Miyawaki A, Furuichi T, Mikoshiba K. 1993. Expression of the metabotropic glutamate receptor mGluR1 alpha and the ionotropic glutamate receptor GluR1 in the brain during the postnatal development of normal mouse and in the cerebellum from mutant mice. J Neurosci Res 36:19–32.

Shirley LT, Messer A. 2004. Early postnatal Purkinje cells from staggerer mice undergo aberrant development in vitro with characteristic morphologic and gene expression abnormalities. Brain Res Dev Brain Res 152:153–157.

Sidman RL, Lane PW, Dickie MM. 1962. Staggerer, a new mutation in the mouse affecting the cerebellum. Science 137:610–612.

Sotelo C. 1990. Cerebellar synaptogenesis: what we can learn from mutant mice. J Exp Biol 153:225–249.

Sotelo C. 2004. Cellular and genetic regulation of the development of the cerebellar system. Prog Neurobiol 72:295–339.

Sotelo C, Arsenio-Nunes ML. 1976. Development of Purkinje cells in absence of climbing fibers. Brain Res 111:289–295.

Sotelo C, Changeux JP. 1974. Transsynaptic degeneration 'en cascade' in the cerebellar cortex of staggerer mutant mice. Brain Res 67:519–526.

Sotelo C, Privat A. 1978. Synaptic remodeling of the cerebellar circuitry in mutant mice and experimental cerebellar malformations. Study "in vivo" and "in vitro." Acta Neuropathol 43:19–34.

Steinmayr M, Andre E, Conquet F, Rondi-Reig L, Delhaye-Bouchaud N, Auclair N, Daniel H, Crepel F, Mariani J, Sotelo C, Becker-Andre M. 1998. Staggerer phenotype in retinoid-related orphan receptor alpha-deficient mice. Proc Natl Acad Sci U S A 95:3960–3965.

Takamori S, Rhee JS, Rosenmund C, Jahn R. 2000. Identification of a vesicular glutamate transporter that defines a glutamatergic phenotype in neurons. Nature 407:189–194.

Takamori S, Rhee JS, Rosenmund C, Jahn R. 2001. Identification of differentiation-associated brain-specific phosphate transporter as a second vesicular glutamate transporter (VGLUT2). J Neurosci 21: RC182.

Takayama C, Nakagawa S, Watanabe M, Mishina M, Inoue Y. 1996. Developmental changes in expression and distribution of the glutamate receptor channel delta 2 subunit according to the Purkinje cell maturation. Brain Res Dev Brain Res 92:147–155.

Tanaka M, Tomita A, Yoshida S, Yano M, Shimizu H. 1994. Observation of the highly organized development of granule cells in rat cerebellar organotypic cultures. Brain Res 641:319–327.

Vogel MW, Sinclair M, Qiu D, Fan H. 2000. Purkinje cell fate in staggerer mutants: agenesis versus cell death. J Neurobiol 42:323–337.

Yamasaki T, Kawaji K, Ono K, Bito H, Hirano T, Osumi N, Kengaku M. 2001. Pax6 regulates granule cell polarization during parallel fiber formation in the developing cerebellum. Development 128:3133–3144.

Yuzaki M. 2003. The delta2 glutamate receptor: 10 years later. Neurosci Res 46:11–22.

Zhou J, Nannapaneni N, Shore S. 2007. Vessicular glutamate transporters 1 and 2 are differentially associated with auditory nerve and spinal trigeminal inputs to the cochlear nucleus. J Comp Neurol 500:777–787.